Cell Reports
Medicine

Article

Pharmacological Inhibition of Acid Sphingomyelinase Prevents Uptake of SARS-CoV-2 by Epithelial Cells

Graphical Abstract

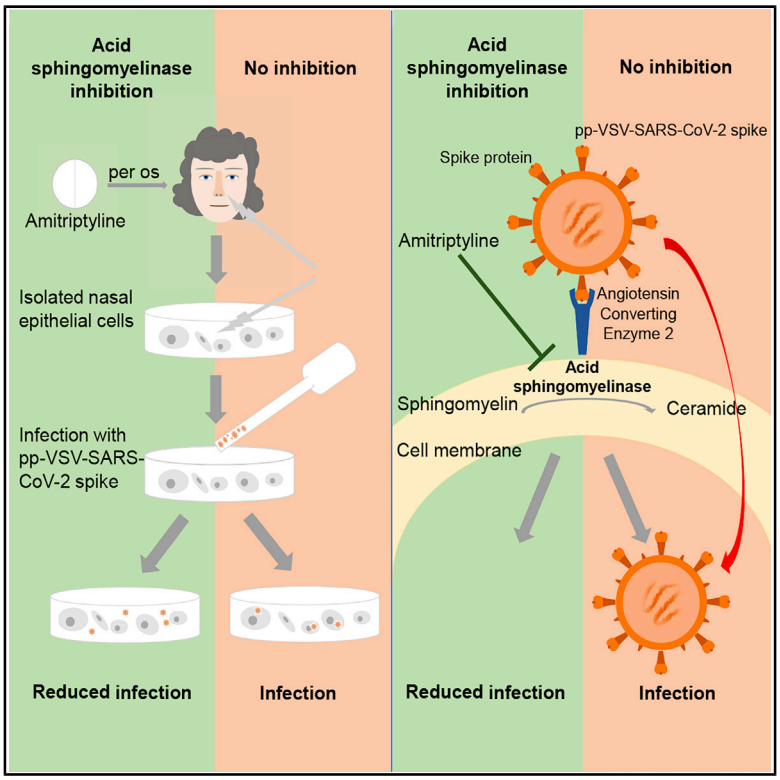

Authors

Alexander Carpinteiro, Michael J. Edwards, Markus Hoffmann, ..., Syed A. Ahmad, Klaus Fassbender, Erich Gulbins

Correspondence

erich.gulbins@uni-due.de

In Brief

Carpinteiro et al. report in a preclinical study that the acid sphingomyelinase/ceramide system is involved in SARS-CoV-2 infections. Functional inhibition of the acid sphingomyelinase/ceramide system with antidepressants reduces infection with authentic or pseudoviral SARS-CoV-2 *in vitro*. Amitriptyline prevents *ex vivo* infection of freshly isolated nasal epithelial cells with pseudoviral SARS-CoV-2.

Highlights

- Pseudoviral SARS-CoV-2 induces the acid sphingomyelinase/ceramide system
- Inhibition of acid sphingomyelinase prevents cellular infection with SARS-CoV-2
- Neutralization of ceramide *in vitro* blocks infection with pseudoviral SARS-CoV-2

Carpinteiro et al., 2020, Cell Reports Medicine *1*, 100142
November 17, 2020
https://doi.org/10.1016/j.xcrm.2020.100142

CellPress

Cell Reports Medicine

CellPress
OPEN ACCESS

Article

Pharmacological Inhibition of Acid Sphingomyelinase Prevents Uptake of SARS-CoV-2 by Epithelial Cells

Alexander Carpinteiro,[1,2] Michael J. Edwards,[3] Markus Hoffmann,[4,5] Georg Kochs,[6] Barbara Gripp,[7] Sebastian Weigang,[6] Constantin Adams,[8] Elisa Carpinteiro,[1] Anne Gulbins,[1] Simone Keitsch,[1] Carolin Sehl,[1] Matthias Soddemann,[1] Barbara Wilker,[1] Markus Kamler,[9] Thomas Bertsch,[10] Karl S. Lang,[11] Sameer Patel,[3] Gregory C. Wilson,[3] Silke Walter,[12] Hartmut Hengel,[6] Stefan Pöhlmann,[4,5] Philipp A. Lang,[13] Johannes Kornhuber,[14] Katrin Anne Becker,[1] Syed A. Ahmad,[3] Klaus Fassbender,[12] and Erich Gulbins[1,3,15,*]

[1]Institute of Molecular Biology, University of Duisburg-Essen, Hufelandstrasse 55, 45122 Essen, Germany
[2]Department of Hematology, University Hospital Essen, University of Duisburg-Essen, Hufelandstrasse 55, 45122 Essen, Germany
[3]Department of Surgery, University of Cincinnati Medical School, 231 Albert Sabin Way, ML0558, Cincinnati, OH 45267, USA
[4]Infection Biology Unit, German Primate Center – Leibniz Institute for Primate Research, Göttingen, Germany
[5]Faculty of Biology and Psychology, University of Göttingen, 37073 Göttingen, Germany
[6]Institute of Virology and Faculty of Medicine, University of Freiburg, Hermann-Herder-Strasse 11, 79104 Freiburg, Germany
[7]Zentrum für Seelische Gesundheit des Kindes- und Jugendalters, Sana-Klinikum Remscheid GmbH, Burger Strasse 211, 42859 Remscheid, Germany
[8]Department of Paediatrics, University Hospital Tuebingen, 72076 Tuebingen, Germany
[9]Department of Thoracic and Cardiovascular Surgery, University Hospital Essen, University of Duisburg-Essen, Hufelandstrasse 55, 45122 Essen, Germany
[10]Institute of Clinical Chemistry, Laboratory Medicine and Transfusion Medicine, Paracelsus Medical University, Nuremberg, Germany
[11]Institute of Immunology, University of Duisburg-Essen, Hufelandstrasse 55, 45147 Essen, Germany
[12]Department of Neurology, University Hospital of the Saarland, Kirrberger Strasse, 66421 Homburg/Saar, Germany
[13]Department of Molecular Medicine II, Medical Faculty, Heinrich Heine University, Universitaetsstrasse 1, 40225 Düsseldorf, Germany
[14]Department of Psychiatry and Psychotherapy, Friedrich-Alexander University Erlangen-Nürnberg (FAU), Schwabachanlage 6, 91054 Erlangen, Germany
[15]Lead Contact
*Correspondence: erich.gulbins@uni-due.de
https://doi.org/10.1016/j.xcrm.2020.100142

SUMMARY

The acid sphingomyelinase/ceramide system plays an important role in bacterial and viral infections. Here, we report that either pharmacological inhibition of acid sphingomyelinase with amitriptyline, imipramine, fluoxetine, sertraline, escitalopram, or maprotiline or genetic downregulation of the enzyme prevents infection of cultured cells or freshy isolated human nasal epithelial cells with severe acute respiratory syndrome coronavirus 2 (SARS-CoV-2) or vesicular stomatitis virus (VSV) pseudoviral particles (pp-VSV) presenting SARS-CoV-2 spike protein (pp-VSV-SARS-CoV-2 spike), a bona fide system mimicking SARS-CoV-2 infection. Infection activates acid sphingomyelinase and triggers a release of ceramide on the cell surface. Neutralization or consumption of surface ceramide reduces infection with pp-VSV-SARS-CoV-2 spike. Treating volunteers with a low dose of amitriptyline prevents infection of freshly isolated nasal epithelial cells with pp-VSV-SARS-CoV-2 spike. The data justify clinical studies investigating whether amitriptyline, a safe drug used clinically for almost 60 years, or other antidepressants that functionally block acid sphingomyelinase prevent SARS-CoV-2 infection.

INTRODUCTION

Infections with a novel member of the *Coronaviridae* family were reported in late 2019 in Wuhan, China.[1] The virus was named severe acute respiratory syndrome coronavirus 2 (SARS-CoV-2). Subsequently, the virus spread globally and is responsible for the coronavirus disease 2019 (COVID-19) pandemic. Infection with SARS-CoV-2 often results in mild respiratory tract disease, but a substantial number of patients also experience severe symptoms and pneumonia, and ~70% of these critically ill patients require intensive care and ventilator treatment, with a mortality rate of 62%.[2] Even when the large number of only mildly affected patients are included, the mortality rates are higher than those associated with seasonal influenza.[3,4]

Cellular infection with SARS-CoV-2 is initiated by the binding of the surface unit S1 of the viral spike glycoprotein to its cellular receptor angiotensin-converting enzyme 2 (ACE2), resulting in cleavage of the viral spike protein by the activity of transmembrane serine protease 2 (TMPRSS2) or cathepsin L and in viral entry.[5–8] Although the binding of the virus to its receptor has

been elucidated in detail,[6–8] the changes that occur in the host cell membrane during viral processing and entry require definition. Membrane changes that mediate viral entry may be a very promising target for preventing the infection.

Previous studies have used replication-deficient vesicular stomatitis virus (VSV) pseudoviral particles (pp-VSV) presenting SARS-CoV-2 spike protein (pp-VSV-SARS-CoV-2 spike) on their surface. Studies have shown that these particles accurately reflect key aspects of the entry of coronavirus into host cells.[5] These particles were previously shown to bind to ACE2 for infectious entry, and entry was inhibited by anti-ACE2 antibodies.[5] Thus, these particles are a bona fide model for studying the events of SARS-CoV-2 entry.

We have previously shown that acid sphingomyelinase and ceramide play an important role in receptor signaling and infection biology.[9,10] Acid sphingomyelinase (EC 3.1.4.12, sphingomyelin phosphodiesterase; optimal pH 5.0) is a glycoprotein that functions as a lysosomal hydrolase, catalyzing the degradation of sphingomyelin to phosphorylcholine and ceramide. Acid sphingomyelinase is present in lysosomes, but because these compartments are constantly recycling to the plasma membrane, it can also be found on the cell surface.[9,10] The activity of acid sphingomyelinase on the cell surface results in the formation of ceramide in the outer leaflet of the cell membrane. The generation of ceramide molecules within the outer leaflet alters the biophysical properties of the plasma membrane because the very hydrophobic ceramide molecules spontaneously associate with each other to form small ceramide-enriched membrane domains that fuse and form large, highly hydrophobic, tightly packed, gel-like ceramide-enriched membrane domains.[10–13] In addition, ceramide has been shown to directly bind to a variety of proteins, including cathepsin D,[14] phospholipase A_2,[15] ceramide-activated protein serine/threonine phosphatases (CAPP),[16] protein kinase C isoforms,[17,18] and microtubule-associated proteins 1A/1B light chain LC3B-II.[19]

Many antidepressants functionally inhibit acid sphingomyelinase activity.[20–25] These cationic amphiphilic drugs indirectly inhibit acid sphingomyelinase activity by displacing the enzyme from lysosomal membranes, in particular intralysosomal vesicles, thereby releasing the enzyme into the lysosomal lumen and causing its partial degradation.[20–25]

We have previously shown that rhinovirus infections activate acid sphingomyelinase and lead to the formation of ceramide and ceramide-enriched membrane domains. Amitriptyline, sertraline, and other functional inhibitors of acid sphingomyelinase activity (FIASMAs) inhibit cellular infection with rhinovirus.[26] Similar observations have been made regarding infections with Ebola virus,[27] demonstrating that amitriptyline and other FIASMAs inhibit infection with Ebola virus *in vitro*.[27]

Because some antidepressants are widely used in clinical practice and have a very favorable safety profile, we investigated whether these drugs could be repurposed to treat or prevent infections with SARS-CoV-2.

Our results show that acid sphingomyelinase is activated within 20 to 30 min after treatment with pp-VSV-SARS-CoV-2 spike; this activation results in the release of ceramide in the outer leaflet of the plasma membrane. In cell culture models, pharmacological or genetic inhibition of acid sphingomyelinase activity or neutralization of surface ceramide prevents the infection of cells with authentic SARS-CoV-2 and pp-VSV-SARS-CoV-2 spike. The addition of exogenous C16 ceramide or acid sphingomyelinase reconstituted the infection with pp-VSV-SARS-CoV-2 spike in cells that had been treated with antidepressants or transfected with short hairpin RNA (shRNA) targeting acid sphingomyelinase. We involved human volunteers in tests of the FIASMA amitriptyline, a safe antidepressant that has been used clinically since 1962. Infection of freshly isolated nasal epithelial cells from volunteers who had been treated with a single dose of 0.5 mg/kg amitriptyline showed almost complete inhibition of the infection of nasal epithelial cells with pp-VSV-SARS-CoV-2 spike particles, an inhibition that lasted for at least 24 h.

RESULTS

Amitriptyline Inhibits SARS-CoV-2 Infections

To determine whether acid sphingomyelinase can be targeted to prevent the infection of cells with SARS-CoV-2, we treated Vero cells with the FIASMA amitriptyline[22–24] or left the cells untreated. We then exposed the cells to pp-VSV-SARS-CoV-2 spike particles and determined infection by measuring the expression of virus-encoded enhanced green fluorescent protein (eGFP) in the infected cells. The results indicate efficient infection of untreated Vero cells with pp-VSV-SARS-CoV-2 spike (Figures 1A and S1). Treating the cells with 5, 10, 20, or 25 μM amitriptyline reduced the infection rate with pp-VSV-SARS-CoV-2 spike by as much as 90%, which was measured as the reduction of the expression of the reporter gene (Figures 1A and S1). Infection of epithelial cells with SARS-CoV-2 has been shown to induce an upregulation of ACE2 expression.[28] We used upregulation of ACE2 expression in Vero cells as an additional readout for infection and for the effects of amitriptyline. Our findings showed that infecting Vero cells with pp-VSV-SARS-CoV-2 spike increased ACE2 expression in Vero cells; this increase was dose-dependently prevented by pretreatment with 10 or 25 μM amitriptyline (Figure 1B). The infection of cells with pp-VSV-G (VSV particles that express the glycoprotein of VSV), which served as a control, was not affected by amitriptyline (Figure 1B).

Fluorescein isothiocyanate (FITC)-Annexin V staining, terminal deoxynucleotidyl transferase dUTP nick end labeling (TUNEL) assays, and staining for the actin cytoskeleton (Figures 1C, 1D, and S2) detected no cytotoxic effects associated with a 24-h treatment with amitriptyline.

Next, we determined whether amitriptyline also affects the infection of human Caco-2 cells with authentic SARS-CoV-2. Amitriptyline-pretreated Caco-2 cells were infected with SARS-CoV-2, and the replication of SARS-CoV-2 was monitored by quantitative real-time RT-PCR by using two separate primer sets and a plaque assay. The results showed that amitriptyline also reduced the infection of human cells with SARS-CoV-2 by approximately 90% (Figure 2).

pp-VSV-SARS-CoV-2 Infection Requires Activation of Acid Sphingomyelinase and Release of Ceramide

The results of these studies suggested that acid sphingomyelinase serves an important function in SARS-CoV-2 infection. To confirm the role of acid sphingomyelinase in infection

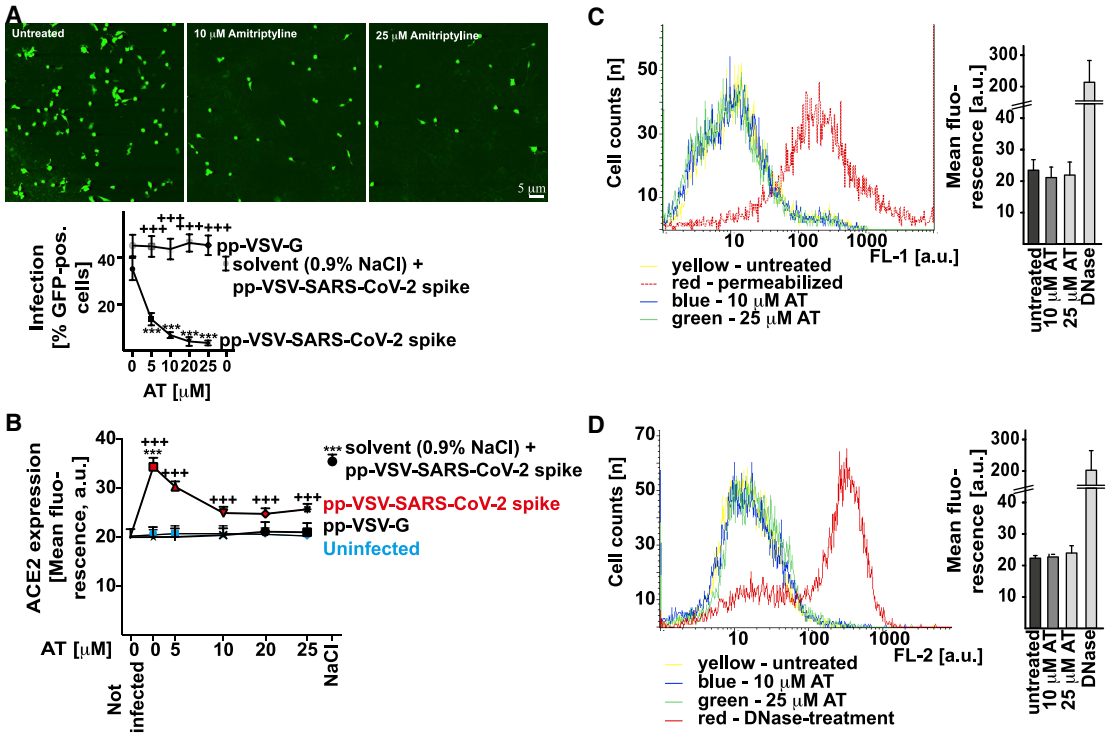

Figure 1. Amitriptyline Prevents Infection with pp-VSV-SARS-CoV-2 Spike

(A) Vero cells were infected for 24 h with vesicular stomatitis virus (VSV) pseudoviral particles presenting severe acute respiratory syndrome coronavirus 2 spike protein (pp-VSV-SARS-CoV-2 spike) or with VSV particles that express the glycoprotein of VSV (pp-VSV-G). Cells were pretreated with amitriptyline (AT) and infected with pp-VSV-SARS-CoV-2 in the presence or absence of 5, 10, 20, or 25 μM AT. The solvent was 0.9% NaCl. AT treatment was initiated 4 h before infection of the pseudoviral particles. Expression of enhanced green fluorescent protein (EGFP) was quantified after 24 h by counting positive cells in 2,000 cells per sample in randomly chosen microscopic fields. Shown are representative fluorescence microscopy results or the means ± SD of the percentage of infected cells from 8 independent experiments. ***$p < 0.001$ compared to infection without AT treatment (0); $^{+++}p < 0.001$ compared between infection with pp-VSV-SARS-CoV-2 spike and pp-VSV-G; ANOVA, followed by post hoc Student's t tests.

(B) Surface expression of angiotensin-converting enzyme 2 (ACE2) was determined by flow cytometry 24 h after infection. Cells were stained with fluorescein isothiocyanate (FITC)-coupled anti-ACE2 antibodies. Shown are the means of the fluorescence ± SD, in random units, from 6 independent experiments. ***$p < 0.001$ compared to not infected; $^{+++}p < 0.001$ compared between infection with pp-VSV-SARS-CoV-2 spike and pp-VSV-G; ANOVA, followed by post hoc Student's t tests.

(C and D) AT did not exhibit cytotoxicity after treatment for 24 h. Cells were exposed for 24 h to 10 μM or 25 μM AT, and toxicity was measured by FITC-Annexin V staining (C) and terminal deoxynucleotidyl transferase dUTP nick end labeling (TUNEL) assay (D). FITC-Annexin V staining and TUNEL assays were analyzed by flow cytometry; staining of cellular actin was analyzed by confocal microscopy. Permeabilized cells served as positive controls for the FITC-Annexin V staining. Permeabilized and DNase-treated cells served as positive controls for TUNEL assays. Shown are representative results from 4 independent studies or the means ± SD of the fluorescence in the flow cytometry studies ($n = 4$); ***$p < 0.001$; ANOVA, followed by post hoc Student's t tests. Results are presented in arbitrary units (a.u.).

with SARS-CoV-2 independent of pharmacological inhibition, we used shRNA-mediated suppression of the expression of acid sphingomyelinase in Caco-2 cells. We confirmed the downregulation of acid sphingomyelinase by measuring the activity of the enzyme in lysates of uninfected cells (Figure 3A). The results showed that genetic downregulation of acid sphingomyelinase prevented infection with pp-VSV-SARS-CoV-2 spike (Figure 3A). Control shRNA constructs had no effect on cellular infection with pp-VSV-SARS-CoV-2 spike. We further tested whether neutral sphingomyelinase may also be involved in cellular infection with SARS-CoV-2. To this end, we transfected Caco-2 cells with shRNA targeting neutral sphingomyelinase 2 and control shRNA. Transfection reduced neutral sphingomyelinase activity by approximately 60% but had no effect on cellular infection with pp-VSV-SARS-CoV-2 spike (Figure 3A).

We next investigated whether infection with pp-VSV-SARS-CoV-2 spike activates the acid sphingomyelinase/ceramide system. The results showed that treating Vero cells with pp-VSV-SARS-CoV-2 spike resulted in rapid activation of acid sphingomyelinase and a concomitant release of ceramide (Figures 3B and 4A).

In contrast, treating Vero cells with pp-VSV lacking SARS-CoV-2 spike or with pp-VSV-G particles did not result in the activation of acid sphingomyelinase or in a release of ceramide (Figures 3B and 4A), a finding indicating that the activation of acid sphingomyelinase and the release of ceramide are specifically induced by the spike protein. Pretreatment of the cells with 5,

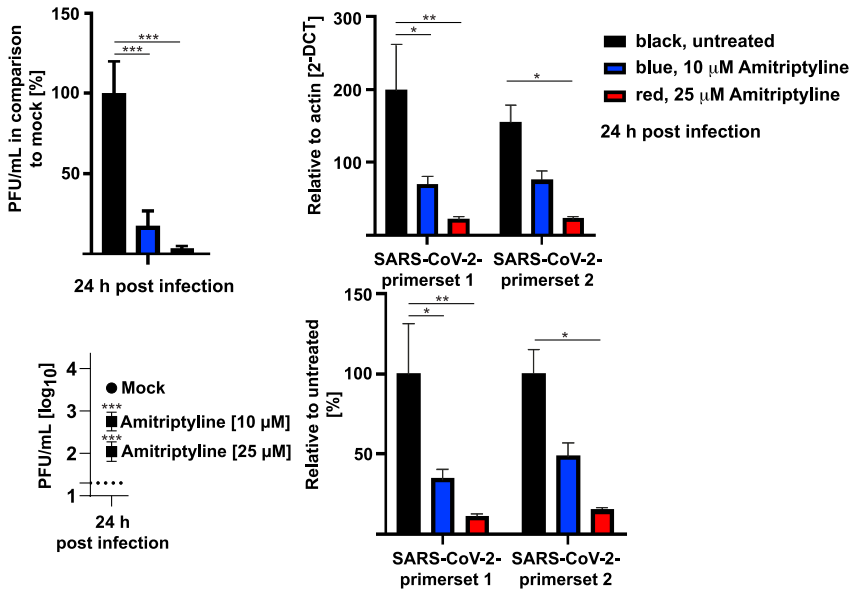

Figure 2. AT Prevents Infection with SARS-CoV-2

Human Caco-2 cells were pretreated with 10 or 25 μM AT for 4 h or left untreated and were infected with SARS-CoV-2 with a multiplicity of infection (MOI) of 0.001 in the presence or absence of AT. The titer of progeny in the culture supernatants was determined 24 h post infection (p.i.) by plaque assay. Viral transcripts were also detected by quantitative real-time RT-PCR with two separate primer sets in the lysates of Caco-2 cells treated as above but infected with a MOI of 0.1 for 24 h. Shown are the means ± SD of 3 experiments; *$p < 0.05$, **$p < 0.01$, ***$p < 0.001$ compared to mock or infected without AT; Dunnets (for plaque-forming units [PFUs]) or Sidak's (for PCR) multiple comparisons test.

10, 20, or 25 μM amitriptyline prevented the activation of acid sphingomyelinase and the release of ceramide upon infection with pp-VSV-SARS-CoV-2 spike for 30 min (Figures 3B and 4A). Controls showed that amitriptyline reduced both the constitutive and the viral-induced activity of acid sphingomyelinase (Figure 3B).

Treating Vero cells with neutralizing antibodies to spike or with recombinant ACE2 protein prevented the activation of acid sphingomyelinase and the release of ceramide upon infection with pp-VSV-SARS-CoV-2 spike (Figures 3B and 4A), a finding that indicated that the interaction of spike with ACE2 mediates the activation of acid sphingomyelinase.

To confirm the formation of ceramide and to determine whether ceramide is released in the plasma membrane after infection, we stained Vero cells prior to and after infection with pp-VSV-SARS-CoV-2 spike with Cy3-coupled anti-ceramide immunoglobulin M (IgM) antibodies and analyzed the cells by flow cytometry. These results revealed the formation of ceramide within the outer leaflet of the plasma membrane upon infection (Figure 4B).

To exclude off-target effects of amitriptyline and shRNA targeting of acid sphingomyelinase, we restored ceramide in amitriptyline-treated or shRNA-transfected cells by adding exogenous C16 ceramide or recombinant human acid sphingomyelinase. The results showed that treatment with C16 ceramide or recombinant human acid sphingomyelinase restored the infection of treated/transfected Vero cells with pp-VSV-SARS-CoV-2 spike (Figure 4C). Controls confirmed that the neutralizing antibodies to spike and the recombinant ACE2 protein used above prevent the infection of cells with pp-VSV-SARS-CoV-2 spike (Figure 4C).

Surface Ceramide Is Required for pp-VSV-SARS-CoV-2 Infection

Neutralization or consumption of surface ceramide by treatment of cells with two separate monoclonal anti-ceramide IgM, i.e., clone S58-9, and a monoclonal anti-ceramide IgG, or neutral ceramidase, respectively, prevented the infection with pp-VSV-SARS-CoV-2 spike (Figure 5A) in a dose-dependent manner, a finding indicating that surface ceramide is required for viral entry.

Many antidepressants functionally inhibit acid sphingomyelinase activity, very likely by interfering with the binding of the protein to lysosomal membranes; this interference results in the release of the enzyme from these membranes and in the degradation of the protein.[20–25] Therefore, we tested whether several other antidepressants, namely imipramine, desipramine, fluoxetine, sertraline, escitalopram, and maprotiline, also inhibit the infection of Vero cells with pp-VSV-SARS-CoV-2 spike. The results showed that all of these drugs at concentrations between 5 μM and 35 μM inhibited acid sphingomyelinase activity (Figure 5B), prevented the entry of pp-VSV-SARS-CoV-2 spike (Figure 5C), and prevented the upregulation of surface ACE2 as marker for the infection (Figure 5D), whereas these drugs exerted no effect on the infection of cells with pp-VSV-G (Figure 5C). Reconstitution of ceramide in the drug-treated Vero cells by the addition of exogenous C16 ceramide restored infection with pp-VSV-SARS-CoV-2 spike (Figure 5C) and did not induce cell death (Figure S3).

Ex vivo Infection of Freshly Isolated Human Nasal Epithelial Cells with pp-VSV-SARS-CoV-2 Spike Is Prevented by Amitriptyline, Anti-ceramide Antibodies, or Neutral Ceramidase

Next, we treated freshly isolated human nasal epithelial cells with amitriptyline, anti-ceramide antibodies, or neutral ceramidase before or upon infection with pp-VSV-SARS-CoV-2 spike. A 60-min pretreatment with 10 μM amitriptyline or the application of anti-ceramide antibodies or neutral ceramidase prevented the infection of freshly isolated nasal epithelial cells with pp-VSV-SARS-CoV-2 spike, as determined by viral uptake (Figure 6A). Reconstitution of ceramide in amitriptyline-treated nasal epithelial cells by the addition of exogenous C16 ceramide restored infection with the pp-VSV-SARS-CoV-2 spike (Figure 6A). Controls demonstrated that amitriptyline reduced the

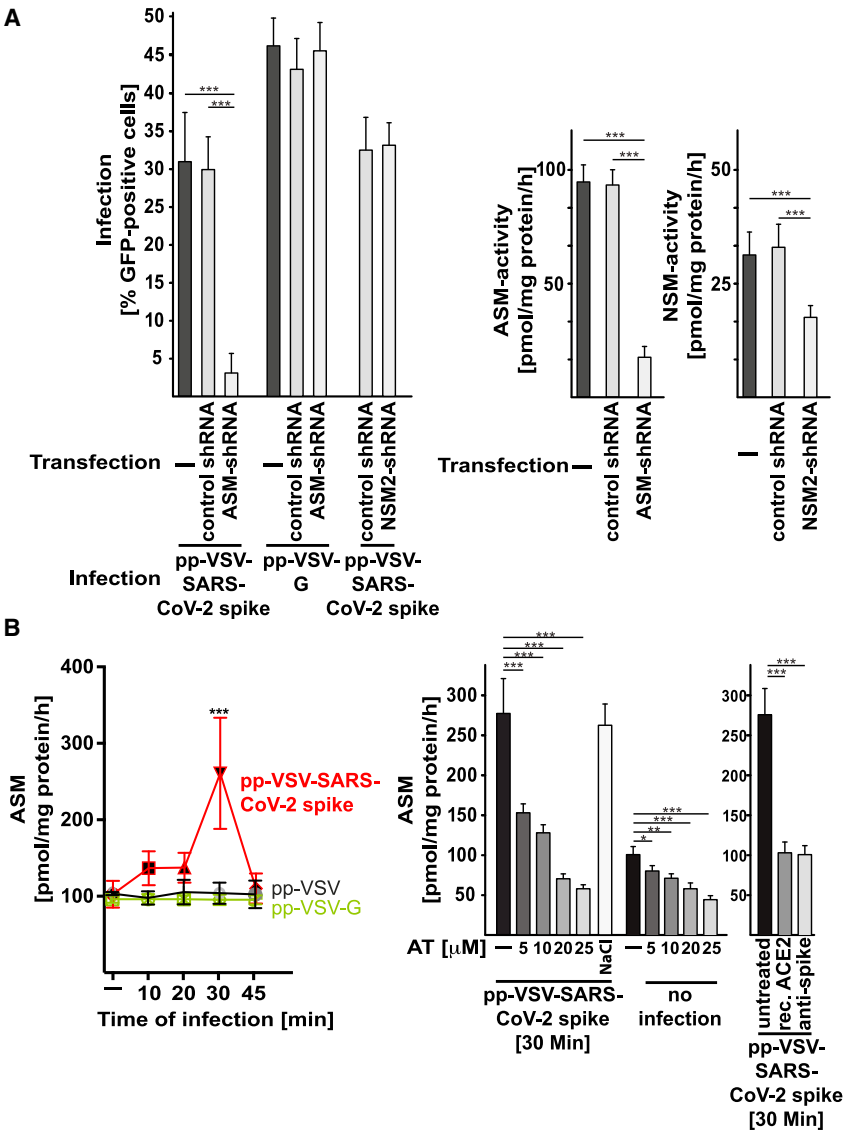

Figure 3. VSV-SARS-CoV-2 Spike Particles Activate and Use the Acid Sphingomyelinase for Infection

(A) Genetic downregulation of acid sphingomyelinase (ASM) with short hairpin RNA (shRNA) prevented infection of Caco-2 cells with pp-VSV-SARS-CoV-2 spike but had no impact on infection with particles that express the pp-VSV-G. Downregulation of neutral sphingomyelinase 2 (NSM2) did not affect the infection of Caco-2 cells with pp-VSV-SARS-CoV-2 spike. Control shRNA did not change the infection of Caco-2 cells by pp-VSV-SARS-CoV-2 spike. Cells were infected with pp-VSV-SARS-CoV-2 spike or pp-VSV-G, and cells positive for EGFP were counted in 2,000 cells per sample. Downregulation of ASM or NSM was confirmed by measuring the activity of the enzymes (right panels).

(B) Vero cells were infected with pp-VSV-SARS-CoV-2 spike, pp-VSV, or pp-VSV-G for the indicated times or were left uninfected. Samples were preincubated with AT or with the solvent (0.9% NaCl) or were left untreated. In addition, recombinant (rec.) ACE2 protein or neutralizing anti-spike antibodies was added prior to and maintained during the infection. Cells were lysed in 250 mM sodium acetate (pH 5.0) and 0.2% NP40. ASM activity was determined by measuring the consumption of [^{14}C] sphingomyelin.

Shown are the means ± SD of the percentage of infected cells or the activity of the ASM or NSM from 6 independent experiments. *p < 0.05, **p < 0.01, ***p < 0.001; ANOVA, followed by post hoc Student's t tests.

activity of acid sphingomyelinase in nasal epithelial cells (Figure 6B).

Amitriptyline Administered *In Vivo* Prevents SARS-CoV-2 Infection of Freshly Isolated Human Nasal Epithelial Cells

Although these findings demonstrate that the infection of Vero cells, Caco-2 cells, and freshly isolated human nasal epithelial cells with pp-VSV-SARS-CoV-2 spike and authentic SARS-CoV-2 can be prevented by treatment with amitriptyline or other antidepressants, with anti-ceramide antibodies, or with neutral ceramidase, they do not demonstrate that clinically used dosages of amitriptyline also block infection with pp-VSV-SARS-CoV-2 spike. To mimic as closely as possible the *in vivo* effect of amitriptyline on infection with pp-VSV-SARS-CoV-2 spike, we treated volunteers with a single oral dose of 0.5 mg/kg amitriptyline. This is a low dose (37.5 mg for a 70-kg volunteer) with no severe adverse effects. We isolated nasal epithelial cells before and 1.5 h and 24 h after the oral administration of amitriptyline and infected these cells by exposing them to pp-VSV-SARS-CoV-2 spike for 60 min. Amitriptyline reduced the activity of acid sphingomyelinase *in vivo* in nasal epithelial cells isolated from the volunteers 1.5 h and 24 h after oral administration. The activity of the enzyme remained reduced for at least 60 min *ex vivo* (Figure 7A). Thus, this protocol allowed us to test the effect of amitriptyline applied *in vivo* on the infection of nasal epithelial cells with pp-VSV-SARS-CoV-2 spike *ex vivo*. The experiments demonstrated that administration of a single oral dose of amitriptyline to volunteers prevented infection of nasal epithelial cells with pp-VSV-SARS-CoV-2 spike (Figures 7B and 7C). The protective effect of amitriptyline administered *in vivo* against infection with pp-VSV-SARS-CoV-2 spike lasted for at least 24 h (Figure 7B). Infection of cells from amitriptyline-treated volunteers was restored by the addition of exogenous C16 ceramide (Figure 7B).

DISCUSSION

In summary, our findings indicate that SARS-CoV-2 activates the acid sphingomyelinase/ceramide pathway and uses this

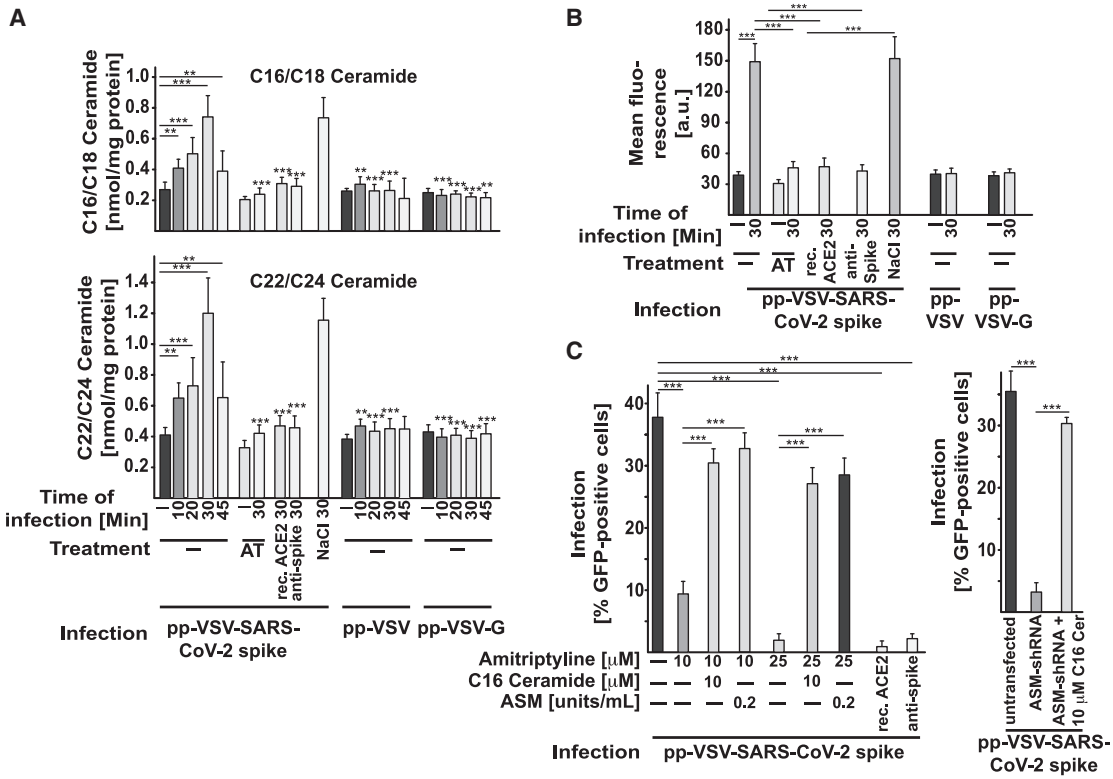

Figure 4. VSV-SARS-CoV-2 Spike Particles Induce Ceramide Formation, Facilitating Infection

(A) To determine ceramide levels, we organically extracted the samples and quantified ceramide levels by using the ceramide kinase method. We quantified C16 (C16-Cer)/C18 ceramide and C22/C24 ceramide. If indicated, cells were preincubated with 5, 10, 20, or 25 μM AT for 4 h before the addition of pp-VSV-SARS-CoV-2 spike. The rec. ACE2 protein or neutralizing anti-spike antibodies were added as above. In addition, cells were infected with pp-VSV or pp-VSV-G. Displayed are the means ± SD of the ceramide concentrations from each 5 independent experiments. **p < 0.01, ***p < 0.001; ANOVA, followed by post hoc Student's t tests, as indicated or compared to the corresponding value without inhibitor.

(B) Flow cytometry reveals the formation of ceramide in the outer leaflet of the cell membrane. Cells were treated with 25 μM AT, each 2 μg rec. ACE2 protein or neutralizing anti-spike antibodies and infected with pp-VSV-SARS-CoV-2 spike. Controls were infected with pp-VSV or pp-VSV-G. Shown are the mean fluorescence values (in a.u.) ± SD of 6 independent flow cytometry studies; ***p < 0.001; ANOVA, followed by post hoc Student's t tests.

(C) Reconstitution of ceramide in Vero cells (left panel) that had been treated with 10 or 25 μM AT or in Caco-2 cells (right panel) transfected with shRNA targeting ASM by the addition of C16-Cer (10 μM) or ASM (0.2 U/mL) during the infection with pp-VSV-SARS-CoV-2 spike restores viral infection of the cells. The rec. ACE2 protein or neutralizing anti-spike antibodies prevented the infection. Displayed are the means ± SD of the percentage of infected cells from 6 independent experiments. ***p < 0.001; ANOVA, followed by post hoc Student's t tests. See also Figure S3.

pathway for infection. Pharmacological or genetic inhibition of acid sphingomyelinase activity prevents infection with authentic SARS-CoV-2 virus or pp-VSV-SARS-CoV-2 spike particles in cell culture models and in freshly isolated human nasal epithelial cells from volunteers treated with amitriptyline and infected *ex vivo*.

Amitriptyline and other drugs with a similar structure and properties have been clinically used for many years (since 1962) to treat patients with depressive disorders. In the volunteer studies, we used a low dose of amitriptyline, i.e., 0.5 mg/kg, which is lower than the dose usually used to treat patients with major depression (75–150 mg/day, i.e., approximately 1–2 mg/kg). At this dose, the drug has only mild effects, such as dry mucosa and tiredness. However, at higher dosages (higher than 100 mg/day, twice the dose we used or higher), amitriptyline and many other antidepressants may induce a cardiac QT elongation as a possible (but rare) adverse effect. QT elongation can result in cardiac arrhythmia and serious cardiac adverse effects.[29] Thus, it may be advisable to perform an electrocardiogram (ECG) before the first administration of amitriptyline or any of the other FIASMAs used here to exclude a pre-existing QT elongation. Amitriptyline and other antidepressants acting as FIASMAs exert no known adverse effects on the immune system.

Our studies demonstrate that even low dosages of amitriptyline provide long-lasting and very efficient protection against infection. Our findings also indicate that other drugs, such as imipramine, desipramine, fluoxetine, sertraline, escitalopram, and maprotiline, with concentrations similar to that of amitriptyline[22] prevent infection with pp-VSV-SARS-CoV-2 spike.

Our studies are strongly supported by a recently pre-printed study[30] that showed a marked beneficial effect of antidepressants on the clinical course of COVID-19. Hospitalized patients receiving antidepressants had a much better outcome, determined as decreased medical necessity of intubation or death, than patients receiving no antidepressants. Best results were

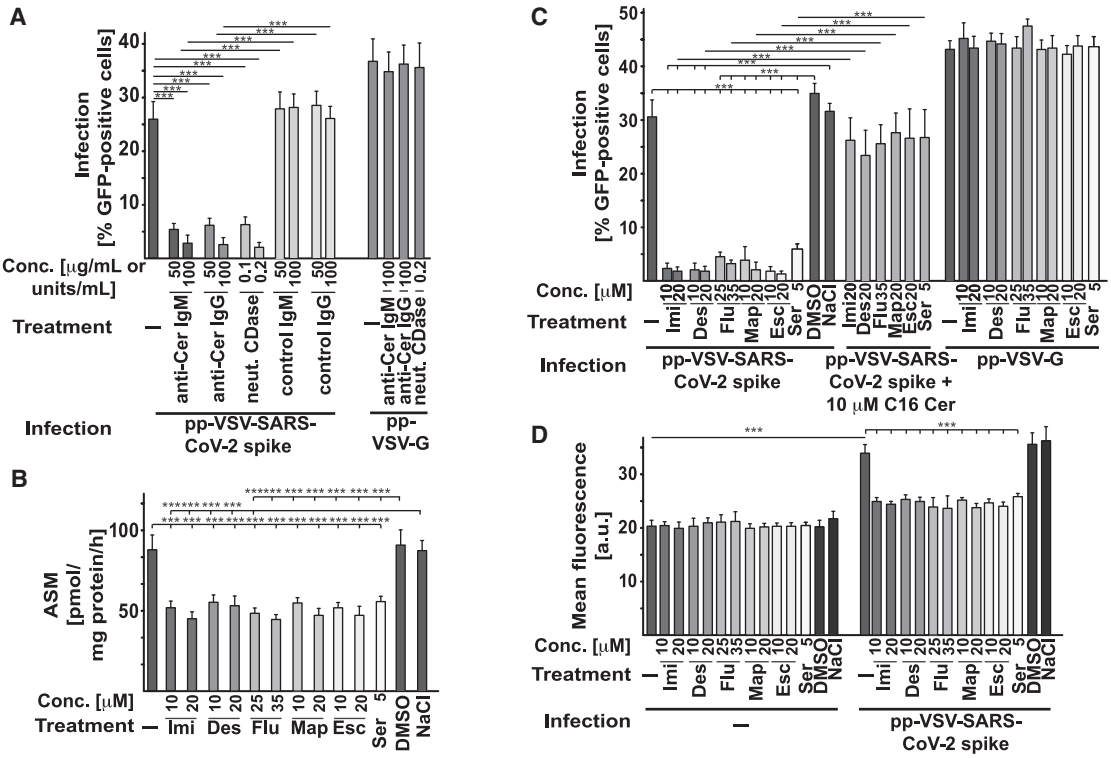

Figure 5. Neutralization of Surface Ceramide or Treatment with Other Antidepressants Prevents Infection with pp-VSV-SARS-CoV-2 Spike

(A) Vero cells were infected with pp-VSV-SARS-CoV-2 spike in the presence or absence of 50 or 100 μg/mL anti-ceramide (anti-Cer) IgM antibodies, clone S58-9, or a monoclonal anti-Cer IgG, or of 0.1 or 0.2 units/mL of neutral ceramidase (neut. CDase) to either neutralize or consume surface ceramide. Infection was measured by the expression of EGFP in the cells. Control IgM or IgG exerted no effect. Anti-Cer antibodies or neut. CDase were without effect on infection with pp-VSV-G. Shown are means ± SD from 5 independent experiments. ***$p < 0.001$; ANOVA, followed by post hoc Student's t tests. Conc., concentration.

(B–D) Incubation of Vero cells with imipramine (Imi), desipramine (Des), fluoxetine (Flu), sertraline (Ser), escitalopram (Esc), or maprotiline (Map) inhibits ASM (B) and prevents the infection of Vero cells with pp-VSV-SARS-CoV-2 spike but not with pp-VSV-G measured as uptake (C) and upregulation of ACE2 expression as measurement for infection (D). Reconstitution of ceramide in treated cells with 10 μM C16-Cer restored infection of the cells with pp-VSV-SARS-CoV-2 spike (C); see also Figure S3. The solvents of the drugs (DMSO or 0.9% NaCl) did not affect ASM activity or viral infection (B–D). Shown are the means ± SD of 6 independent experiments. ***$p < 0.001$; ANOVA, followed by post hoc Student's t tests.

obtained with venlafaxine, fluoxetine, escitalopram, and mirtazapine, drugs that were also shown in the present study to inhibit acid sphingomyelinase and ceramide release upon pp-VSV-SARS-CoV-2 spike infection. It is important to note that the dose of antidepressants used in this retrospective study was not optimized. Amitriptyline was used at a medium dose of 26 mg/day, which is a rather low dose. Amitriptyline is often used at these low dosages for sedation and not as an antidepressant, whereas other drugs such as fluoxetine and escitalopram are always used as antidepressants and applied at higher dosages.

Furthermore, fluoxetine also inhibits SARS-CoV-2 replication,[31] an effect that was not investigated in the present study, because the pseudoviral particles do not replicate.

Amitriptyline and many other antidepressants are weak bases that are protonated in lysosomes and thereby trapped in lysosomes, but they also localize in acidic subcompartments of the cell membrane. Because of their physicochemical properties (for instance for amitriptyline: high lipophilicity and weak basicity; logP = 4.92, acid dissociation constant pKa = 9.4; https://go.drugbank.com/), these drugs accumulate in acidic intracellular compartments.[32] This accumulation leads to a high tissue concentration and accordingly to a high volume of distribution (for instance for amitriptyline: distribution volume Vd = 16 L/kg; https://go.drugbank.com/). Thus, high tissue concentrations of these drugs can be detected in all organs. In fact, the highest uptake of amitriptyline among all tissues with a lung/blood concentration gradient of approximately 50 is found in the lungs of mice and rats.[33,34] In humans, even higher concentration gradients have been found between the lung and blood.[35] Because of the particularly high accumulation in the lung, the antiviral *in vitro* concentrations (up to 25 μM) that we found to be effective are likely to be achieved with conventional oral therapy of amitriptyline. We also expect a considerably longer elimination half-life of amitriptyline in lung tissue than in blood because of the high concentration of these drugs in deep compartments, such as lysosomes.

The organic ring system of amitriptyline and other FIASMAs may bind to the lipid membrane, whereas the protonated tertiary amine displaces acid sphingomyelinase from lysosomal membranes or from the plasma membrane within acidic subdomains. Thus, these weak bases do not directly inhibit acid sphingomyelinase activity but rather functionally inhibit it. This mode of action

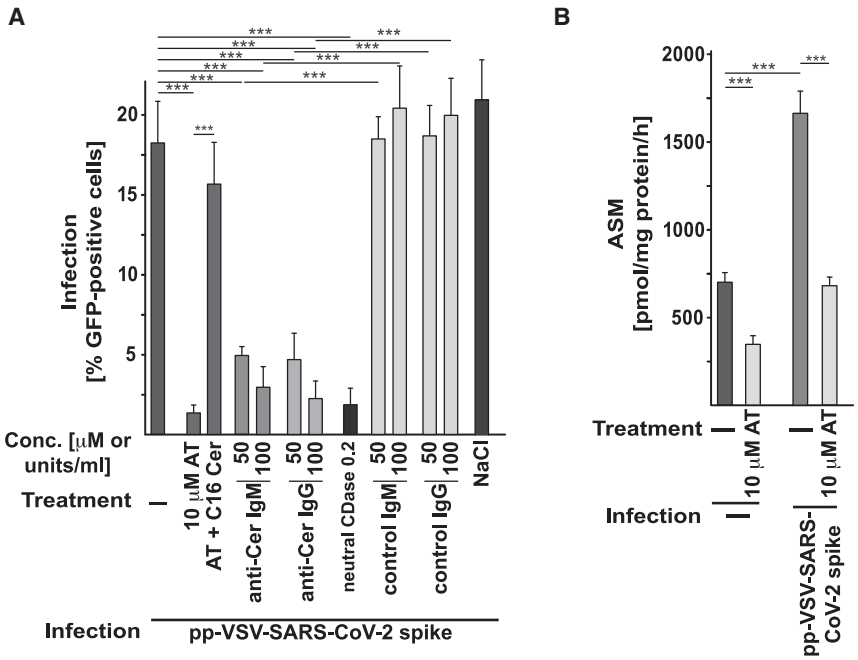

Figure 6. Infection of Freshly Isolated Human Nasal Epithelial Cells Is Prevented by *Ex Vivo* Treatment with AT, Anti-Cer Antibodies, or neut. CDase

(A) Freshly isolated human nasal epithelial cells were infected with pp-VSV-SARS-CoV-2 spike for 60 min. Anti-Cer antibodies (IgM or IgG) or neut. CDase were co-applied with the virus. AT (10 μM) was applied for 60 min before the infection and was also present during the infection. All of these treatments blocked the infection of freshly isolated human nasal epithelial cells with pp-VSV-SARS-CoV-2 spike. Control IgM, IgG, or 0.9% NaCl (solvent for AT) exerted no effect. Ceramide was reconstituted in AT-treated nasal epithelial cells with 10 μM C16-Cer; this reconstitution restored the infection of the cells with pp-VSV-SARS-CoV-2 spike.

(B) AT reduced ASM activity in nasal epithelial cells upon infection.

Shown are the means ± SD of 6 (A) or 5 (B) independent experiments. ***$p < 0.001$; ANOVA, followed by post hoc Student's t tests.

also explains why antidepressants do not completely inhibit acid sphingomyelinase activity and do not induce severe adverse effects in clinical use.

In addition, our studies indicate that the administration of anti-ceramide antibodies or neutral ceramidase also protects against SARS-CoV-2 infections. Anti-ceramide antibodies and neutral ceramidase are not approved for clinical use but could be easily tested for systemic or local adverse effects before the treatment of SARS-CoV-2 infections. Furthermore, both anti-ceramide antibodies and neutral ceramidase could potentially be administered by inhalation or as a nasal spray to prevent SARS-CoV-2 infections.

The molecular mechanisms of how ceramide mediates the infection of epithelial cells with SARS-CoV-2 remain to be determined. Ceramide has been shown to directly activate several enzymes and to form large, highly hydrophobic ceramide-enriched membrane domains that serve to re-organize receptor and signaling molecules.[10–13] It remains to be determined whether SARS-CoV-2 also induces these platforms and whether ceramide and/or these platforms are required for the internalization or activation of TMPRSS2 and cathepsin L that mediate the processing of spike required for fusion with the cell membrane.[36]

High ceramide levels have been linked with hypertension and obesity,[37,38] two of the most important risk factors for the development of serious infections with SARS-CoV-2. It is tempting to speculate that the increased levels of ceramide associated with these diseases sensitize cells to infection with SARS-CoV-2 and thereby contribute to the development of serious infections.

The results with volunteers demonstrated that the *in vivo* administration of amitriptyline is sufficient to reduce acid sphingomyelinase activity and to prevent infection of nasal epithelial cells *in vitro*. It is now necessary to confirm the effects of antidepressants in SARS-CoV-2 infections in clinical studies investigating prophylactic and therapeutic effects of these drugs for COVID-19. We hope that our study stimulates further studies that support or refute the clinical use of antidepressants for the prevention or treatment of SARS-CoV-2 infections.

Limitations of Study

The findings were generated from experimental *in vitro* model systems. Infections were performed *ex vivo*, and experiments in animal models are required to confirm the data *in vivo*. Although we showed that infection of human epithelial cells and different human cell lines with SARS-CoV-2 and pp-VSV-SARS-CoV-2-spike particles is significantly reduced by treatment with several antidepressants and genetic inhibition of the acid sphingomyelinase, this does not necessarily reflect the clinical situation in COVID-19. Clinical data/studies are required to define the clinical use of antidepressants for the treatment of COVID-19. Clinical studies are also required to elucidate the best antidepressant for a potential treatment for COVID-19 patients. Finally, further mechanistic studies are necessary to elucidate how the acid sphingomyelinase and ceramide are involved in infection.

STAR★METHODS

Detailed methods are provided in the online version of this paper and include the following:

- KEY RESOURCES TABLE
- RESOURCE AVAILABILITY
  - Lead Contact
  - Materials Availability
  - Data and Code Availability
- EXPERIMENTAL MODEL AND SUBJECT DETAILS
  - Human subjects
  - Primary cells

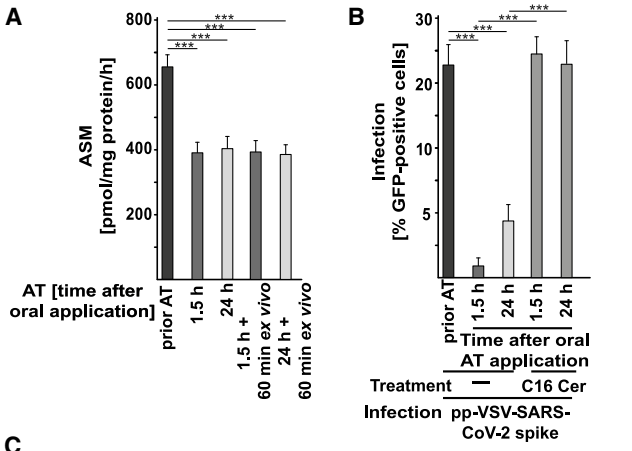

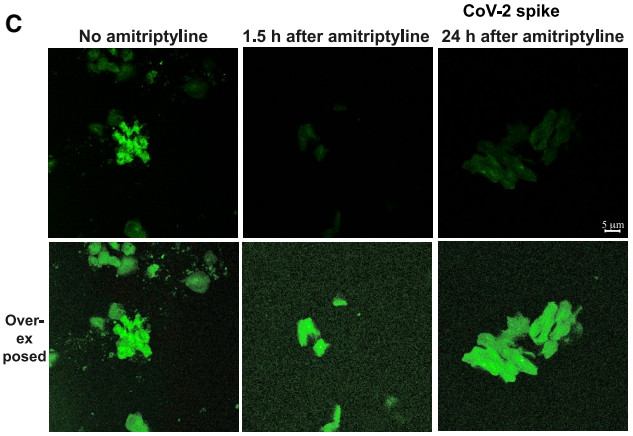

Figure 7. *In Vivo* Administration of AT Prevents Infection of Nasal Epithelial Cells with pp-VSV-SARS-CoV-2 Spike *Ex Vivo*

Volunteers were orally treated with 0.5 mg/kg AT. Nasal epithelial cells were isolated from volunteers before and 1.5 h and 24 h after administration of AT.

(A) Activity of ASM was determined by measurement of the consumption of [^{14}C]sphingomyelin in aliquots of freshly isolated nasal epithelial cells or after an additional 1-h culture *ex vivo*.

(B) After isolation, nasal epithelial cells were infected for 1 h, with pp-VSV-SARS-CoV-2 spike and washed. The expression of EGFP was determined after 24 h in at least 500 epithelial cells per sample in randomly chosen microscopic fields. Ceramide in nasal epithelial cells isolated from volunteers who had taken AT was reconstituted with 10 µM C16-Cer. This reconstitution restored the infection of the cells with pp-VSV-SARS-CoV-2 spike. The percentage of infected nasal epithelial cells is displayed.

(C) Shown is a typical result from 6 independent infection studies with nasal epithelial cells from volunteers before and after oral administration of AT. The bottom panel shows an over-exposed microphotograph to visualize all cells.

Shown are the means ± SD from 6 volunteers. ***$p < 0.001$; ANOVA, followed by post hoc Student's t tests.

SUPPLEMENTAL INFORMATION

Supplemental Information can be found online at https://doi.org/10.1016/j.xcrm.2020.100142.

ACKNOWLEDGMENTS

The study was supported by Deutsche Forschungsgemeinschaft, Germany, grants Gu-335-35/1 and GU-335-38/1 to Erich Gulbins and Federal Ministery of Science (BMBF), RAPID Consortium grant 01KI1723D to Stefan Pöhlmann.

AUTHOR CONTRIBUTIONS

E.G. initiated the studies. E.G., M.J.E., A.C., B.G., S.A.A., J.K., Silke Walter, Sameer Patel, G.C.W., T.B., M.K., C.A., and K.F. contributed to the planning of the experiments. M.H. and Stefan Pöhlmann provided the pp-VSV-SARS-CoV-2 spike. S. Weigang, G.K., H.H., and P.A.L. performed and discussed the SARS-CoV-2 experiments. E.G., A.C., K.A.B., E.C., A.G., B.G., and K.S.L. performed the human studies. J.K., S.W., K.F., B.G., and E.G. determined the dosages of antidepressants. E.G. performed all other infection experiments and measurements of enzymes and ceramide. M.S., C.S., S.K., and B.W. contributed to the immune staining studies. All authors have read and commented on the manuscript.

DECLARATION OF INTERESTS

The authors declare no competing financial interests.

Received: June 29, 2020
Revised: September 23, 2020
Accepted: October 22, 2020
Published: October 29, 2020

REFERENCES

1. Zhou, P., Yang, X.L., Wang, X.G., Hu, B., Zhang, L., Zhang, W., Si, H.R., Zhu, Y., Li, B., Huang, C.L., et al. (2020). A pneumonia outbreak associated with a new coronavirus of probable bat origin. Nature *579*, 270–273.
2. Yang, X., Yu, Y., Xu, J., Shu, H., Xia, J., Liu, H., Wu, Y., Zhang, L., Yu, Z., Fang, M., et al. (2020). Clinical course and outcomes of critically ill patients with SARS-CoV-2 pneumonia in Wuhan, China: a single-centered, retrospective, observational study. Lancet Respir. Med. *8*, 475–481.
3. World Health Organization. Coronavirus disease (COVID-19): similarities and differences with influenza.https://www.who.int/emergencies/diseases/novel-coronavirus-2019/question-and-answers-hub/q-a-detail/q-a-similarities-and-differences-covid-19-and-influenza?gclid=EAIaIQobChMIz5b_0bem6QIVFuDtCh1s1QwHEAAYASAAEgJomPD_BwE.
4. John Hopkins University. Mortality analyses.https://coronavirus.jhu.edu/data/mortality.

5. Hoffmann, M., Kleine-Weber, H., Schroeder, S., Krüger, N., Herrler, T., Erichsen, S., Schiergens, T.S., Herrler, G., Wu, N.H., Nitsche, A., et al. (2020). SARS-CoV-2 cell entry depends on ACE2 and TMPRSS2 and is blocked by a clinically proven protease inhibitor. Cell *181*, 271–280.e8.

6. Wrapp, D., Wang, N., Corbett, K.S., Goldsmith, J.A., Hsieh, C.L., Abiona, O., Graham, B.S., and McLellan, J.S. (2020). Cryo-EM structure of the 2019-nCoV spike in the prefusion conformation. Science *367*, 1260–1263.

7. Lan, J., Ge, J., Yu, J., Shan, S., Zhou, H., Fan, S., Zhang, Q., Shi, X., Wang, Q., Zhang, L., and Wang, X. (2020). Structure of the SARS-CoV-2 spike receptor-binding domain bound to the ACE2 receptor. Nature *581*, 215–220.

8. Wang, Q., Zhang, Y., Wu, L., Niu, S., Song, C., Zhang, Z., Lu, G., Qiao, C., Hu, Y., Yuen, K.Y., et al. (2020). Structural and functional basis of SARS-CoV-2 entry by using human ACE2. Cell *181*, 894–904.e9.

9. Grassmé, H., Jekle, A., Riehle, A., Schwarz, H., Berger, J., Sandhoff, K., Kolesnick, R., and Gulbins, E. (2001). CD95 signaling via ceramide-rich membrane rafts. J. Biol. Chem. *276*, 20589–20596.

10. Grassmé, H., Jendrossek, V., Riehle, A., von Kürthy, G., Berger, J., Schwarz, H., Weller, M., Kolesnick, R., and Gulbins, E. (2003). Host defense against Pseudomonas aeruginosa requires ceramide-rich membrane rafts. Nat. Med. *9*, 322–330.

11. Gulbins, E., and Kolesnick, R. (2003). Raft ceramide in molecular medicine. Oncogene *22*, 7070–7077.

12. Kolesnick, R.N., Goñi, F.M., and Alonso, A. (2000). Compartmentalization of ceramide signaling: physical foundations and biological effects. J. Cell. Physiol. *184*, 285–300.

13. Nurminen, T.A., Holopainen, J.M., Zhao, H., and Kinnunen, P.K.J. (2002). Observation of topical catalysis by sphingomyelinase coupled to microspheres. J. Am. Chem. Soc. *124*, 12129–12134.

14. Heinrich, M., Wickel, M., Schneider-Brachert, W., Sandberg, C., Gahr, J., Schwandner, R., Weber, T., Saftig, P., Peters, C., Brunner, J., et al. (1999). Cathepsin D targeted by acid sphingomyelinase-derived ceramide. EMBO J. *18*, 5252–5263.

15. Huwiler, A., Johansen, B., Skarstad, A., and Pfeilschifter, J. (2001). Ceramide binds to the CaLB domain of cytosolic phospholipase A2 and facilitates its membrane docking and arachidonic acid release. FASEB J. *15*, 7–9.

16. Dobrowsky, R.T., and Hannun, Y.A. (1993). Ceramide-activated protein phosphatase: partial purification and relationship to protein phosphatase 2A. Adv. Lipid Res. *25*, 91–104.

17. Müller, G., Ayoub, M., Storz, P., Rennecke, J., Fabbro, D., and Pfizenmaier, K. (1995). PKC zeta is a molecular switch in signal transduction of TNF-alpha, bifunctionally regulated by ceramide and arachidonic acid. EMBO J. *14*, 1961–1969.

18. Huwiler, A., Fabbro, D., and Pfeilschifter, J. (1998). Selective ceramide binding to protein kinase C-alpha and -delta isoenzymes in renal mesangial cells. Biochemistry *37*, 14556–14562.

19. Dany, M., Gencer, S., Nganga, R., Thomas, R.J., Oleinik, N., Baron, K.D., Szulc, Z.M., Ruvolo, P., Kornblau, S., Andreeff, M., and Ogretmen, B. (2016). Targeting FLT3-ITD signaling mediates ceramide-dependent mitophagy and attenuates drug resistance in AML. Blood *128*, 1944–1958.

20. Hurwitz, R., Ferlinz, K., and Sandhoff, K. (1994). The tricyclic antidepressant desipramine causes proteolytic degradation of lysosomal sphingomyelinase in human fibroblasts. Biol. Chem. Hoppe Seyler *375*, 447–450.

21. Kölzer, M., Werth, N., and Sandhoff, K. (2004). Interactions of acid sphingomyelinase and lipid bilayers in the presence of the tricyclic antidepressant desipramine. FEBS Lett. *559*, 96–98.

22. Kornhuber, J., Tripal, P., Reichel, M., Terfloth, L., Bleich, S., Wiltfang, J., and Gulbins, E. (2008). Identification of new functional inhibitors of acid sphingomyelinase using a structure-property-activity relation model. J. Med. Chem. *51*, 219–237.

23. Gulbins, E., Palmada, M., Reichel, M., Lüth, A., Böhmer, C., Amato, D., Müller, C.P., Tischbirek, C.H., Groemer, T.W., Tabatabai, G., et al. (2013). Acid sphingomyelinase-ceramide system mediates effects of antidepressant drugs. Nat. Med. *19*, 934–938.

24. Gulbins, A., Schumacher, F., Becker, K.A., Wilker, B., Soddemann, M., Boldrin, F., Müller, C.P., Edwards, M.J., Goodman, M., Caldwell, C.C., et al. (2018). Antidepressants act by inducing autophagy controlled by sphingomyelin-ceramide. Mol. Psychiatry *23*, 2324–2346.

25. Breiden, B., and Sandhoff, K. (2019). Emerging mechanisms of drug-induced phospholipidosis. Biol. Chem. *401*, 31–46.

26. Grassmé, H., Riehle, A., Wilker, B., and Gulbins, E. (2005). Rhinoviruses infect human epithelial cells via ceramide-enriched membrane platforms. J. Biol. Chem. *280*, 26256–26262.

27. Miller, M.E., Adhikary, S., Kolokoltsov, A.A., and Davey, R.A. (2012). Ebolavirus requires acid sphingomyelinase activity and plasma membrane sphingomyelin for infection. J. Virol. *86*, 7473–7483.

28. Ziegler, C.G.K., Allon, S.J., Nyquist, S.K., Mbano, I.M., Miao, V.N., Tzouanas, C.N., Cao, Y., Yousif, A.S., Bals, J., Hauser, B.M., et al. (2020). SARS-CoV-2 receptor ACE2 is an Interferon-stimulated gene in human airway epithelial cells and is detected in specific cell subsets across tissues. Cell *181*, 1016–1035.e19.

29. Unterecker, S., Pfuhlmann, B., Kopf, J., Kittel-Schneider, S., Reif, A., and Deckert, J. (2015). Increase of heart rate and QTc by Amitripytline, but not by Venlafaxine, is correleated to serum concentration. J. Clin. Psychopharmacol. *35*, 460–463.

30. Hoertel, N., Sanchez Rico, M., Verney, R., Beeker, N., Jannot, A.-S., Neuraz, A., Salamanca, E., Paris, N., Daniel, C., Gramfort, A., et al. (2020). Association between SSRI antidepressant use and reduced risk of intubation or death in hospitalized patients with coronavirus disease 2019: a multicenter retrospective observational study. medRxiv. https://doi.org/10.1101/2020.07.09.20143339.t.

31. Zimniak, M., Kirschner, L., Hilpert, H., Seibel, J., and Bodem, J. (2020). The serotonin reuptake inhibitor Fluoxetine inhibits SARS-CoV-2. bioRxiv. https://doi.org/10.1101/2020.06.14.150490.

32. Trapp, S., Rosania, G.R., Horobin, R.W., and Kornhuber, J. (2008). Quantitative modeling of selective lysosomal targeting for drug design. Eur. Biophys. J. *37*, 1317–1328.

33. Cassano, G.B., Sjöstrand, S.E., and Hansson, E. (1965). Distribution and fate of C-14-amitriptyline in mice and rats. Psychopharmacology (Berl.) *8*, 1–11.

34. Hilberg, T., Mørland, J., and Bjørneboe, A. (1994). Postmortem release of amitriptyline from the lungs; a mechanism of postmortem drug redistribution. Forensic Sci. Int. *64*, 47–55.

35. Bynum, N.D., Poklis, J.L., Gaffney-Kraft, M., Garside, D., and Ropero-Miller, J.D. (2005). Postmortem distribution of tramadol, amitriptyline, and their metabolites in a suicidal overdose. J. Anal. Toxicol. *29*, 401–406.

36. Matsuyama, S., Nagata, N., Shirato, K., Kawase, M., Takeda, M., and Taguchi, F. (2010). Efficient activation of the severe acute respiratory syndrome coronavirus spike protein by the transmembrane protease TMPRSS2. J. Virol. *84*, 12658–12664.

37. Yu, J., Pan, W., Shi, R., Yang, T., Li, Y., Yu, G., Bai, Y., Schuchman, E.H., He, X., and Zhang, G. (2015). Ceramide is upregulated and associated with mortality in patients with chronic heart failure. Can. J. Cardiol. *31*, 357–363.

38. Smith, E.L., and Schuchman, E.H. (2008). The unexpected role of acid sphingomyelinase in cell death and the pathophysiology of common diseases. FASEB J. *22*, 3419–3431.

39. Berger Rentsch, M., and Zimmer, G. (2011). A vesicular stomatitis virus replicon-based bioassay for the rapid and sensitive determination of multi-species type I interferon. PLoS One *6*, e25858.

40. Kleine-Weber, H., Elzayat, M.T., Wang, L., Graham, B.S., Müller, M.A., Drosten, C., Pöhlmann, S., and Hoffmann, M. (2019). Mutations in the spike protein of Middle East respiratory syndrome coronavirus transmitted in Korea increase resistance to antibody-mediated neutralization. J. Virol. *93*, e01381-18.

STAR★METHODS

KEY RESOURCES TABLE

REAGENT or RESOURCE	SOURCE	IDENTIFIER
Antibodies		
Anti-VSV-G (I1, produced from CRL-2700 mouse hybridoma cells)	ATCC	Cat# CRL-2700; RRID: CVCL_G654
Rabbit monoclonal anti-SARS-Cov-2 Spike 1	Sino Biological	Cat# 40150-R-007; RRID: AB_2827979
Mouse anti-ceramide IgM antibody clone S85-9	Glycobiotech	Cat# MAB_0014
Mouse monoclonal anti-ceramide IgG	Antibody Res. Corp.	Cat# 111583
Cy3-coupled donkey anti-mouse IgM $F(ab)_2$ fragment	Jackson Immunoresearch	Cat# 715-166-020
Goat anti-ACE2 antibody	R&D	Cat# AF933
FITC-coupled donkey anti-goat antibody	Jackson Immunoresearch	Cat# 705-096-147
Bacterial and Virus Strains		
SARS-CoV-2 (isolate Muc-IMB-1)	Bundeswehr Institute of Microbiology, Munich, Germany	Isolate Muc-IMB-1
VSV*ΔG-FLuc	Laboratory of Stefan Pöhlmann, ref. [5]	n/a
Chemicals, Peptides, and Recombinant Proteins		
Recombinant human neutral ceramidase	R&D	Cat# 3557 AH
Recombinant ACE2	Abcam	Cat# ab273687
Recombinant acid sphingomyelinase	R&D	Cat# 5348-PD-010
Amitriptyline, Tablets	Neuraxpharm	PZN 3343120
Amitriptyline	Sigma-Aldrich	Cat# A8404
Imipramine	Sigma-Aldrich	Cat# I0899
Desipramine	Sigma-Aldrich	Cat# D3900
Sertraline	Sigma-Aldrich	Cat# S6319
Escitalopram	Sigma-Aldrich	Cat# E4786
Maprotiline	Sigma-Aldrich	Cat# M9651
Fluoxetine	Sigma-Aldrich	Cat# 56296-78-7
C16-ceramide	Avanti Polar Lipids	Cat# 860516
[^{14}C]sphingomyelin	Perkin Elmer,	Cat# #NEC 663010UC
[^{32}P]γATP	Hartmann Radiochemicals	Cat# SCP-501-150
DAG kinase	ENZO	Cat# BML-SE100
FITC-Annexin V	Roche	Cat#11 828 681 001
Cell dissociation buffer	GIBCO	Cat#13151-014
Critical Commercial Assays		
TUNEL kit (*in situ* cell death detection kit TMR red)	Roche	Cat#12156792910
Experimental Models: Cell Lines		
Human nasal epithelial cells	Healthy volunteers	This study
Caco-2 (human colon epithelial cells)	ATCC	Cat# HTB-37; RRID CVCL_0025
Vero (monkey kidney epithelial cells)	ATCC	Cat# CCL-81; RRID CVCL_0059
HEK293T (human embryonic kidney cells)	DSMZ	Cat# ACC-635; RRID CVCL_0063
Oligonucleotides		
SRBR Green 1 fwd: GCCTCTTCTCGTTCCTCATCAC	Merck	n/a

(*Continued on next page*)

Continued

REAGENT or RESOURCE	SOURCE	IDENTIFIER
SRBR Green 1 rev: AGCAGCATCACCGCCATTG	Merck	n/a
SRBR Green 2 fwd: AGCCTCTTCTCGTTCCTCATCAC	Merck	n/a
SRBR Green 2 rev: CCGCCATTGCCAGCCATTC	Merck	n/a
shRNA targeting acid sphingomyelinase	Santa Cruz Inc.	Cat# sc-41650-SH
shRNA targeting neutral sphingomyelinase	Santa Cruz Inc.	Cat# sc-62655-SH
Recombinant DNA		
Synthetic, codon optimized (humanized) SARS-2-S	ThermoFisher Scientific (GeneArt)	n/a
Plasmid: pCAGGS-VSV-G	Laboratory of Stefan Pöhlmann, ref. [5]	n/a
Plasmid: pCG1-SARS-2-S	Laboratory of Stefan Pöhlmann, ref. [5]	n/a
Software and Algorithms		
G*Power (version 3.1.7)	University of Duesseldorf	https://www.gpower.hhu.de/
Leica LCS (version 2.61)	Leica	https://www.leica.com/
Adobe Illustrator 2020 (version 24.3)	Adobe	https://www.adobe.com/
Microsoft Office 2011 (version 16.16.7)	Microsoft Corporation	http://www.microsoft.com
GraphPad Prism (version 8.2.1)	GraphPad Software	https://www.graphpad.com/

RESOURCE AVAILABILITY

Lead Contact

Further information and requests for resources and reagents should be directed to and will be fulfilled by the lead contact, Erich Gulbins (erich.gulbins@uni-due.de).

Materials Availability

This study did not generate new unique reagents.

Data and Code Availability

The published article includes all datasets generated or analyzed during the study.

EXPERIMENTAL MODEL AND SUBJECT DETAILS

Human subjects

Human nasal epithelial cells were obtained from 6 healthy volunteers, 4 women and 2 men. Their ages were 20, 21, 43, 48, 54, and 56. We did not observe any differences in infection between cells from women or men. Sample size was planned for the continuous variable difference in viral uptake and was based on two-sided Wilcoxon-Mann-Whitney tests using G*Power Version 3.1.7, University of Duesseldorf, Germany. Nasal epithelial cells were obtained from all subjects prior and after oral application of amitriptyline and, thus, all subjects were included in both arms (untreated versus treated) of the study.

The experiments were approved by the ethic committee of the University Hospital Essen under the number 20-9348-BO.

Primary cells

We obtained nasal epithelial cells from these volunteers immediately before oral administration of 0.5 mg/kg amitriptyline (Neuraxpharm, Germany) and again 1.5 h and 24 h after administration of amitriptyline. The cells were removed from the nasal mucosa by inserting a small brush into the nose (approximately 1.5-2 cm deep). The brush was gently rotated within the nose. Nasal epithelial cells were released from the brush and suspended immediately in 1 mL HEPES/saline (H/S; 132 mM NaCl, 20 mM HEPES [pH 7.4], 5 mM KCl, 1 mM $CaCl_2$, 0.7 mM $MgCl_2$, 0.8 mM $MgSO_4$) and immediately used for infection.

Cell lines

Vero cells (ATCC CCL-81; monkey kidney epithelial cells) were cultured in Dulbecco's Modified Eagle Medium (DMEM) supplemented with 10 mM HEPES (pH 7.4; Carl Roth GmbH, Karlsruhe, Germany), 2 mM L-glutamine, 1 mM sodium pyruvate, 100 μM

nonessential amino acids, 100 U/mL penicillin, 100 μg/mL streptomycin (all from Invitrogen, city, country), and 10% FCS (PAA Laboratories GmbH, Coelbe, Germany).

Caco-2 colon epithelial cells (ATCC HTB-37) were cultured in DMEM supplemented as described above.

METHOD DETAILS

Pseudoviral particles

Pseudotyped viral particles based on a replication-deficient VSV that codes for eGFP and firefly luciferase instead of parental VSV-G (VSV*ΔG-FLuc),[39] were generated according to a previously published protocol.[40] At 24 h after transfection by the calcium-phosphate method, HEK293T cells transiently expressing either SARS-2-S or VSV-G were inoculated with VSV-G-trans-complemented VSV*ΔG-FLuc for 1 h at 37°C and 5% CO_2, after which the inoculum was removed and cells were washed with phosphate-buffered saline (PBS). Finally, the cells were transferred to fresh culture medium and were incubated at 37°C and 5% CO_2. For cells expressing SARS-2-S, the culture medium was supplemented with anti-VSV-G antibody (I1, mouse hybridoma supernatant from American Type Culture Collection [ATCC] CRL-2700) for inactivation of residual VSV-G-trans-complemented VSV*ΔG-FLuc. At 16 h after inoculation, the culture supernatants were harvested, and cellular debris was pelleted by centrifugation (4,000 × g, 4°C, 10 min). The clarified supernatants were used for the experiments.

Infection of nasal epithelial cells

For infection freshly isolated nasal epithelial cells were pelleted by centrifugation, and resuspended in minimum essential medium (MEM) supplemented with 10% fetal calf serum (FCS) containing pp-VSV-SARS-CoV-2 spike particles. Cells were infected for 60 min, washed in H/S, and cultured for 24 h to allow expression of the eGFP encoded by the particles. Infection was analyzed with a Leica TCS SL confocal microscope (Mannheim, Germany) by counting the percentage of eGFP-positive epithelial cells in at least 500 epithelial cells per sample in randomly chosen microscopic fields.

A further aliquot of the nasal epithelial cells was immediately shock frozen in liquid nitrogen after removal for determination of acid sphingomyelinase activity (see below).

Ex vivo treatment of nasal epithelial cells

Nasal epithelial cells were also obtained from untreated volunteers as described above and were treated with 10 μM amitriptyline (Sigma; # A 8404) dissolved in 0.9% NaCl, anti-ceramide or control antibodies, neutral ceramidase (see below) or left untreated for 60 min *ex vivo* and then infected with pp-VSV-SARS-CoV-2 spike particles for 60 min. Cells were then washed and further incubated for 24 h to allow expression of eGFP. Infection was analyzed as above.

Infection of Vero lines

Vero cells were grown to subconfluency for 24 h on glass coverslips in a 24-well plate before measurement of the uptake of the pp-VSV-SARS-CoV-2 spike or pp-VSV-G particles. Amitriptyline (5, 10, 20, or 25 μM) was dissolved in 0.9% NaCl and added to the cells 4 h before the addition of pp-VSV-SARS-CoV-2 spike or pp-VSV-G particles. Because amitriptyline binds to serum proteins, we reduced the concentration of FCS in the medium to 1% during the 4 h preincubation period. Controls were also incubated in serum-reduced medium, but without amitriptyline. The medium was then removed, 250 μL of a cell culture supernatant containing pp-VSV-SARS-CoV-2 or pp-VSV-G particles and, if indicated, amitriptyline (5, 10, 20 or 25 μM) was added, and the cells were incubated for 8 h. In addition, we added 2 μg/mL anti-spike (S1) antibody (Sino Biological, #40150-R-007) or 2 μg/mL recombinant ACE2 (Abcam; # ab273687) to the cells 30 min before adding the viral particles. The concentrations were maintained during the infection. We then removed the supernatants, added DMEM medium supplemented as above, and incubated the cells for an additional 12 h to allow expression of eGFP. The medium was removed; cells were washed once in H/S, fixed in 1% paraformaldehyde (PFA) buffered with PBS (pH 7.3) for 10 min, washed, embedded in Mowiol, and analyzed with a Leica TCS-SL confocal microscope equipped with a 40 × lens and Leica LCS software version 2.61. We counted EGFP-positive cells in 2000 cells per sample in randomly chosen microscopic fields. In addition, fixed cells were stained with propidiumiodide (0.5 μg/mL) for 2 min to visualize cells.

Flow cytometry of surface ACE2 as measurement for infection

Cells were cultured in 24-well plates, treated with 25 μM amitriptyline or solvent (0.9% NaCl) for 4 h or left untreated, infected with pp-VSV-SARS-CoV-2, pp-VSV or pp-VSV-G particles, the medium was removed and cells were collected with a cell dissociation buffer (GIBCO; #13151-014). Samples were washed twice in H/S, stained at 4°C for 45 min with 1 μg/mL anti-ACE2 antibodies (1:1000, R&D, #AF933) ceramide antibodies, washed twice in ice-cold H/S, stained with FITC-coupled donkey anti-goat antibodies (1:1000; Jackson Immunoresearch; #705-096-147) for 45 min at 4°C, washed and analyzed by flow cytometry with a BD Calibur.

Infection with SARS-CoV-2

Approximately 10^6 Caco-2 colon epithelial cells (ATCC HTB-37) were cultured in 6-well plates in DMEM supplemented and pretreated with amitriptyline or were left untreated in DMEM with 1% FCS for 4 h, as described above. Cells were then infected with 1000 plaque-forming units (PFU) of SARS-CoV-2 (isolate Muc-IMB-1, obtained from the Bundeswehr Institute of Microbiology,

Munich, Germany) in 1 mL medium for 1.5 h at 37°C, corresponding to a multiplicity of infection (MOI) of 0.001. Cells were then washed with DMEM and further incubated with 2.5 mL DMEM, 1% FCS, and 20 mM HEPES (pH 7.4) containing 10 μM or 25 μM amitriptyline or left untreated. Viral titers in the culture supernatants were determined after 24 h with plaque assays. Studies using RT-qPCR for quantification of the infection followed the same protocol, except that the MOI was increased to 0.1. The primer pairs used for RTqPCR were purchased from Merck: SYBR Green 1, fwd-GCCTCTTCTCGTTCCTCATCAC and rev- AGCAGCATC ACCGCCATTG; and SYBR Green 2, fwd- AGCCTCTTCTCGTTCCTCATCAC and rev- CCGCCATTGCCAGCCATTC. The results were reproduced by two independent co-authors of the manuscript.

Neutralization of ceramide

To neutralize ceramide in Vero cells or nasal epithelial cells, we added 50 or 100 μg/mL of the anti-ceramide IgM antibody clone S85-9 (Glycobiotech; MAB_0014) or of a mouse monoclonal anti-ceramide IgG (Antibody Res. Corp.; #111583), or either 0.1 or 0.2 units/mL of neutral ceramidase (R&D, #3557 AH) to the cells, which were then immediately infected with pp-VSV-SARS-CoV-2 spike particles for 60 min. Controls were incubated with irrelevant IgM or IgG antibodies (Dako). Cells were then washed, cultured for 24 h, and analyzed for infection as above.

FITC-Annexin V binding

Cells were treated for 4 h with 10 or 25 μM amitriptyline in DMEM supplemented with 1% FCS as above. Incubation was then continued for 20 h in DMEM containing 10% FCS. Cells were trypsinized, washed in H/S, stained for 15 min with FITC-Annexin V (Roche), and analyzed by flow cytometry. Controls were permeabilized for 5 min with 0.1% Triton X-100 at room temperature before incubation with FITC-Annexin V.

TUNEL studies

Vero cells were treated with 10 or 25 μM amitriptyline as described for FITC-Annexin V staining. Cells were trypsinized, washed with PBS, fixed in 4% PFA buffered in PBS (pH 7.4) for 10 min, washed in PBS, permeabilized with 0.1% Triton X-100 in 0.1% sodium citrate for 5 min at room temperature, and washed. Next, the TUNEL reaction was performed exactly as instructed by the vendor (Roche, #12156792910) using recombinant terminal deoxynucleotidyl transferase (rTdT; EC 2.7.7.31) and tetramethyl rhodamine (TMR) red-labeled nucleotides. Samples were analyzed by flow cytometry. Positive controls were incubated with recombinant micrococcal nuclease or DNase I (3000 U/ml) for 10 min at 22°C before the TUNEL reaction.

Actin staining

Vero cells were grown on glass coverslips, treated with 10 or 25 μM amitriptyline as described above, washed, fixed for 10 min in 1% PFA buffered in PBS (pH 7.3), washed, permeabilized for 5 min with 0.1% Triton X-100 at room temperature, washed and stained with FITC-Phalloidin for 12 h at 4°C. The samples were washed again and embedded in Mowiol. Cells were then analyzed by confocal microscopy on a Leica TCS SL confocal microscope equipped with a 40 × lens and Leica LCS software version 2.61.

Genetic downregulation of sphingomyelinase

The expression of acid or neutral sphingomyelinase in Caco-2 cells was downregulated by transfection with commercial shRNA targeting acid sphingomyelinase (Santa Cruz Inc.; # sc-41650-SH) or neutral sphingomyelinase (Santa Cruz Inc.; # sc-62655-SH). Cells were transiently transfected by electroporation at 400 V with 5 pulses, 3 msec each, with a BTX electroporator. Control cells were transfected with an irrelevant shRNA (Santa Cruz Inc., # sc-108060). Dead cells were removed by Ficoll gradient centrifugation, and cells were cultured for 36 h before infection with pp-VSV-SARS-CoV-2 spike. Downregulation of acid or neutral sphingomyelinase was confirmed by measuring the activity of the enzyme in transfected, control-transfected, and untransfected cells.

Acid sphingomyelinase activity

To determine acid sphingomyelinase activity, we grew Vero or Caco-2 cells in 24-well plates. Cells were pretreated with amitriptyline for 4 h or transfected as above or were left untreated. The cells were washed in H/S and infected with 250 μL of cell culture supernatant containing pp-VSV-SARS-CoV-2 spike or control pp-VSV particles for 10 to 45 min. Untreated cells were incubated with DMEM that was supplemented as above. Amitriptyline was added at 5 - 25 μM as above. The incubation was terminated by removing the supernatants, and the cells were immediately lysed in 250 mM sodium acetate (pH 5.0) and 1% NP40 for 5 min. The lysates were removed from the plates and diluted to 0.2% NP40 in 250 mM sodium acetate (pH 5.0). Next, we added 0.05 μCi [^{14}C]sphingomyelin (52 mCi/mmol; Perkin Elmer, #NEC 663010UC) per sample. The substrate [^{14}C]sphingomyelin was dried for 10 min in a SpeedVac, resuspended in 250 mM sodium acetate (pH 5.0) and 0.1% NP40, and sonicated for 10 min in a bath sonicator before it was added to the samples. The samples were incubated for 30 min at 37°C with shaking at 300 rpm. The enzymatic reaction was terminated by extraction in 4 volumes of $CHCl_3$:CH_3OH (2:1, v/v), the samples were centrifuged, and an aliquot of the upper aqueous phase was scintillation-counted to determine the release of [^{14}C]phosphorylcholine from [^{14}C]sphingomyelin.

To determine the effect of amitriptyline on the activity of the acid sphingomyelinase in nasal epithelial cells, we washed the cells once in H/S after infection. Pellets were immediately shock-frozen, lysed in 250 mM sodium acetate (pH 5.0) and 1% NP40 for 5 min, and processed as above.

Neutral sphingomyelinase activity

Vero cells were infected with pp-VSV-SARS-CoV-2 spike for 5, 10, 20, 30, 45, or 60 min or were left untreated; lysed in a buffer containing 100 mM TrisHCl (pH 7.4), 5 mM $MgCl_2$, 2.5 mM DTT, 0.2% Triton and 10 μg/ml each of aprotinin and leupeptin; sonicated; and incubated with 0.02 μCi [^{14}C]sphingomyelin per sample for 30 min at 37°C. Samples were processed as described for acid sphingomyelinase.

Measurement of ceramide

Cells were treated as above with 25 μM amitriptyline for 4 h or left untreated and then washed in H/S. Next, 250 μL of the cell culture supernatant containing pp-VSV-SARS-CoV-2 spike or control pp-VSV or pp-VSV-G particles was added as above for a period of 10 to 45 min. Amitriptyline (25 μM) was immediately added again after the addition of the pseudoviral particles. Untreated cells were incubated with DMEM supplemented as above. The medium was removed, and cells were lysed in 200 μL H_2O, scraped from the plates, and extracted in $CHCl_3$:CH_3OH:1N HCl (100:100:1, v/v/v). Samples were centrifuged for 5 min at 14,000 rpm. The lower phase was collected, dried, and resuspended in 20 μL of a detergent solution (7.5% [w/v] n-octyl glucopyranoside, 5 mM cardiolipin in 1 mM diethylenetriaminepentaacetic acid [DTPA]). Micelles were obtained by bath sonication for 10 min and used for the kinase reaction, which was initiated by adding 70 μL of a reaction mixture containing 10 μL diacylglycerol (DAG) kinase (GE Healthcare Europe, Munich, Germany), 0.1 M imidazole/HCl (pH 6.6), 0.2 mM DTPA (pH 6.6), 70 mM NaCl, 17 mM $MgCl_2$, 1.4 mM ethylene glycol tetraacetic acid, 2 mM dithiothreitol, 1 μM adenosine triphosphate (ATP), and 5 μCi [^{32}P]γATP (6000 Ci/mmol; Hartmann Radiochemicals, Braunschweig, Germany). The kinase reaction was performed for 60 min at room temperature with 300 rpm shaking and was terminated by the addition of 1 mL $CHCl_3$:CH_3OH:1N HCl (100:100:1, v/v/v), 170 μL buffered saline solution (135 mM NaCl, 1.5 mM $CaCl_2$, 0.5 mM $MgCl_2$, 5.6 mM glucose, 10 mM HEPES [pH 7.2]), and 30 μL of a 100 mM EDTA solution. Phases were separated, and the lower phase was collected. The samples were then dried in a SpeedVac, separated on Silica G60 thin-layer chromatography (TLC) plates with chloroform/acetone/methanol/acetic acid/H_2O (50:20:15:10:5, v/v/v/v/v), and developed with a Fuji phosphoimager. Ceramide amounts were determined by comparison with a standard curve using C16 to C24 ceramides as substrates.

Other antidepressants

To test the effects of other antidepressants on the infection of Vero cells with pp-VSV-SARS-CoV-2 spike or pp-VSV-G, we treated Vero cells for 4 h with 10 or 20 μM imipramine (Sigma-Aldrich; # I 0899), 10 or 20 μM desipramine (Sigma-Aldrich, # D 3900), 5 μM sertraline (Sigma-Aldrich; # S 6319), 10 or 20 μM escitalopram (Sigma-Aldrich; # E 4786), 10 or 20 μM maprotiline (Sigma-Aldrich; # M 9651) or 25 or 35 μM fluoxetine (Sigma-Aldrich; # 56296-78-7). Amitriptyline, desipramine and imipramine, were dissolved in 0.9% NaCl, all other antidepressants in DMSO with a final concentration of 0.1% DMSO. Controls were 0.9% NaCl or 0.1% DMSO. We then determined the activity of acid sphingomyelinase or infected the cells with pp-VSV-SARS-CoV-2 spike or pp-VSV-G particles for 24 h and then determined the expression of eGFP or the expression of ACE2 on the cell surface as measurements for infection as above.

Ceramide reconstitution

Cells were treated with 10 or 20 μM amitriptyline, 10 or 20 μM imipramine, 10 or 20 μM desipramine, 5 μM sertraline, 10 or 20 μM escitalopram, or 10 or 20 μM maprotiline or 25 or 35 μM fluoxetine for 4 h or transfected with shRNA targeting the acid sphingomyelinase as above and infected with pp-VSV-SARS-CoV-2 spike, after which 10 μM C16 ceramide (Avanti Polar Lipids; # 860516) or 0.2 U/mL recombinant acid sphingomyelinase (specific activity: 1700 pmol/min/μg; R&D, #5348-PD-010) was immediately added. C16 ceramide was resuspended in cell culture medium and sonicated for 10 min in a bath sonicator before use. We then determined viral uptake as above.

Flow cytometry of surface ceramide

Vero cells were cultured in 24-well plates, treated with 25 μM amitriptyline or solvent (0.9% NaCl) for 4 h as above, each 2 μg/mL recombinant ACE2 or anti-spike antibodies or left untreated, and infected with pp-VSV-SARS-CoV-2, pp-VSV or pp-VSV-G particles for 30 min. The cells were collected with a cell dissociation buffer (GIBCO; #13151-014), washed twice in H/S, stained at 4°C for 45 min with 1 μg/mL anti-ceramide antibodies, clone S85-9, washed twice in ice-cold H/S, stained with Cy3-coupled donkey anti-mouse IgM F(ab)$_2$ fragments (1:1000; Jackson Immunoresearch; #715-166-020) for 45 min at 4°C, washed and analyzed by flow cytometry with a BD Calibur.

QUANTIFICATION AND STATISTICAL ANALYSIS

Data are expressed as arithmetic means ± SD. For the comparison of continuous variables from independent groups we used one-way ANOVA followed by post hoc Student's t tests for all pairwise comparisons and the Bonferroni correction for multiple testing. The *p* values for the pairwise comparisons were calculated after Bonferroni correction. All values were normally distributed. Statistical significance was set at the level of $p \leq 0.05$ (two-tailed). Sample size planning for the continuous variable *in vivo* experiments was based on two-sided Wilcoxon-Mann-Whitney tests (free software: G*Power Version 3.1.7, University of Duesseldorf, Germany). Investigators were blinded to the identity of the samples in all microscopy experiments.

DATA AVAILABILITY STATEMENTS

All data are available upon request from the authors. Authors confirm that all data are included in the manuscript.

ADDITIONAL RESOURCES

n/a